

SCIENTIFIC REPORTS



OPEN

Study on regeneration of waste powder activated carbon through pyrolysis and its adsorption capacity of phosphorus

Yi Li¹, Hailan Jin¹, Wenbo Liu¹, Hang Su¹, Yao Lu² & Jianfen Li²

The regeneration of WPAC through pyrolysis and its adsorption capacity of phosphorus were studied. The optimum conditions for WPAC regeneration were 650 °C and 2 h which resulted in a recovery of BET surface and total pore volume with a value of 1161.4 m²/g and 1.2176 m³/g. WPAC had a maximum PO₄³⁻-P adsorption capacity of 9.65 mg/g which was 48.93% of PAC, while RWPAC had a maximum PO₄³⁻-P adsorption capacity of 15.31 mg/g which was 77.64% of PAC. The kinetic analysis revealed that Langmuir model could well describe the adsorption process of PAC, WPAC and RWPAC on PO₄³⁻-P and the PO₄³⁻-P adsorption followed the pseudo-second-order model.

Phosphorous is the main component causing the eutrophication in lakes, coastal areas, and other confined water bodies. Many technologies including adsorption, biological nutrient removal and precipitation have been applied to remove phosphorus from wastewater due to the increasingly stringent regulations on phosphorus discharge. The adsorption process is one of the most efficient methods of removing phosphorus from wastewater.

Powder activated carbons (PACs) is the most widely used adsorbent due to its large surface area, well developed pore structure and adsorption capacity^{1,2}. However, during their applications, PACs will become progressively saturated with adsorbates, and therefore lose their adsorption capacity. Usually those waste PACs (WPAC) are incinerated or discharged which will cause a secondary source of pollution³. Compared with incineration or other treatments, regeneration of WPAC which can restore their adsorption capacity is more significant for the waste re-utilization and environmental protection.

There are several kinds of methods for activated carbon regeneration like oxidizing regeneration⁴, thermal regeneration^{5,6}, microwave regeneration^{7,8} and biological regeneration^{9,10}. However, biological regeneration and oxidizing method are either time-consuming or uneconomic. Although microwave has been utilized to regenerate activated carbon while the application is still very limited. The most widely used regeneration method is thermal regeneration. Three PACs with widely different BET areas were evaluated to determine the effects of thermal regeneration on their physical and chemical properties by Clifford¹¹. PAC weight% recoveries were in the range of 60–80%, and the recovery of wastewater adsorption capacity regularly exceeded 100% for all carbons. The pyrolysis and combustion characteristics of a waste oil absorbing activated carbon were investigated using a thermogravimetric analyzer under heating rate of 10 °C/min from 25 °C to 1000 °C. The results indicated that the pyrolytic process is divided into three stages while the incineration process of the waste oil absorbing activated carbon is in four phases¹². The regeneration process of WPAC is depended on a large number of parameters like regeneration duration and the temperature which will make great influence on adsorption capacity recovery percentage and weight loss percentage. Therefore, the analysis of the regeneration process and the evaluation of regeneration effect are strongly required.

Pyrolysis is regarded to be a promising approach in which organic matters can be decomposed and converted into biochar, bio-oil and permanent gases in the absence of oxygen during 150~700 °C¹³. The focus of the present work is to regenerate the WPAC by pyrolysis. The effects of regeneration on the characteristic of WPAC through pyrolysis were analyzed. Meanwhile the performance for the phosphorous adsorption by WRPAC was also investigated.

¹College of Material Science and Engineering, Northeast Forestry University, Harbin, 150040, PR China.

²School of Chemical and Environmental Engineering, Wuhan Polytechnic University, Wuhan, 430073, PR China. Correspondence and requests for materials should be addressed to H.J. (email: 1820395578@qq.com) or J.L. (email: jianfenli_whpu@126.com)

Materials and Method

Materials. The fresh PAC and WPAC used for the experiment were obtained from a saccharin plant in XiangYang, HuBei, China. PAC was used as the adsorbent to deal with the saccharin wastewater with a mean value of COD (18.2 g/L), $\text{NH}_4^+\text{-N}$ (50 mg/L) and pH(3.6). PAC was previously boiled with deionized water for 1.5 h in order to remove the other impurities. Then PAC and WPAC were dried to constant weight for the subsequent use.

Regeneration procedures. The regeneration of WPAC was carried out in a vertical pyrolysis furnace. Experiments were conducted using batch method to determine the optimal temperature and regeneration time. To determine the optimal temperature of pyrolysis, about 10 g of the sample was pyrolysed under 500 mL/min N_2 flow at heating rate of $10^\circ\text{C}/\text{min}$ from 25°C to the designated temperature (550°C , 600°C , 650°C , 700°C and 750°C) with a regeneration duration ranged from 0.5 to 3.0 h. The atmosphere was also maintained during the heating up and cooling-down intervals. The loss rate of pyrolysis η (LRP) was calculated according to the Eq. (1).

$$\eta = \frac{M_1 - M_2}{M_1} \times 100\% \quad (1)$$

where M_1 was the mass of WPAC before regeneration, M_2 was the mass of WPAC after regeneration.

Phosphorus adsorption capacity of WPAC. Experiments were carried out to investigate the adsorption capacity of PAC, WPAC and RWPAC on phosphorus.

Adsorption isotherms. Artificial wastewater was synthesized by adding a certain amount of KH_2PO_4 into distilled water. Equilibrium sorption studies were conducted in a 50 mL erlenmeyer flasks each containing 30 mL wastewater. 0.02 g PAC, WPAC or RWPAC with a corresponding initial concentration of wastewater (10, 40, 80, 120, 200 and 400 $\text{mgPO}_4^{3-}\text{-P/L}^{-1}$, respectively). The flasks were agitated in a shaker at 150 rpm and 20°C for 4 h to reach equilibrium. The $\text{PO}_4^{3-}\text{-P}$ adsorption capacity per unit mass of adsorbent at equilibrium, q_e ($\text{mgPO}_4^{3-}\text{-P/g}$), was calculated by Eq. (2):

$$q_e = (C_0 - C)V/(1000 M) \quad (2)$$

where V was the volume of the solution (mL); M was the mass of adsorbent (g); C_0 and C were the concentration of $\text{PO}_4^{3-}\text{-P}$ before and after the adsorption (mg/L).

Adsorption isotherms model. Adsorption isotherms is necessary to describe the adsorption capacity of PAC, WPAC and RWPAC. The equilibrium concentration of PAC, WPAC and RWPAC in the solution could be helpful for the analysis and the design of the sorption systems. In this study, two adsorption isotherms were developed by Langmuir model (Eq. (3)) and Freundlich model (Eq. (4))^{14,15}.

$$\frac{C_e}{q_e} = \frac{1}{q_{\max}k_L} + \frac{C_e}{q_{\max}} \quad (3)$$

$$\log q_e = \log k_F + \frac{1}{n} \log C_e \quad (4)$$

where k_L is the Langmuir isotherm constant (L/mg), q_{\max} represent the maximum $\text{PO}_4^{3-}\text{-P}$ adsorption capacity of PAC, WPAC and RWPAC (mg/g). k_F is the Freundlich isotherm constant which indicates the maximum adsorption capacity (mg/g). $1/n$ is the Freundlich isotherm constant which is dimensionless. C_e is the equilibrium concentration of the adsorbed substance in the liquid phase (mg/L) and q_e is the constant that indicates the maximum adsorbate quantity of the adsorbent (mg/g).

Analytical methods. TG and derivative thermogravimetric (DTG) analysis was carried out with a thermogravimetric analyzer (TG/DTA SDT Q600, USA). The chemical functional groups in the samples were investigated by FTIR (Nicolet 6700, Thermo Fisher Scientific, USA). The surface area and pore characteristics of WPAC were analyzed using BET (ASAP2020 HD88, USA). Phosphate concentration was determined by the colorimetric method. All of the tests were conducted in 3 replications, and the mean values were used.

Results and Discussion

Influence of regeneration conditions. The regeneration temperature and duration of pyrolysis are important parameters for WPAC regeneration, as organic matters can be decomposed at high temperature. Besides, the regeneration temperature and duration also make influence on the weight loss percentage. The influences of pyrolysis duration and pyrolysis temperature on the LRP of WPAC were displayed on Fig. 1. As seen in Fig. 1, LRP increased with the extend of pyrolysis time for all pyrolysis temperatures. The maximum LRP was obtained at 2 h. After 2 h, there was not obvious difference on LRP. For the same pyrolysis time, LRP increased at the region of $550\text{--}650^\circ\text{C}$ while litter difference was caused at the region of $650\text{--}750^\circ\text{C}$. The maximum LRP (24.5%) was reached at 650°C which indicated that the decomposition of organic matters adsorbed on the WPAC was completely finished. Therefore, the optimum regeneration conditions were 650°C and 2 h with the concern of energy consumption and economic for regeneration.

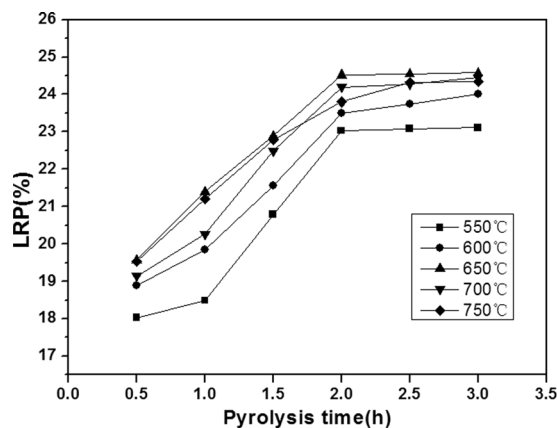


Figure 1. Influence of regeneration conditions on the LRP.

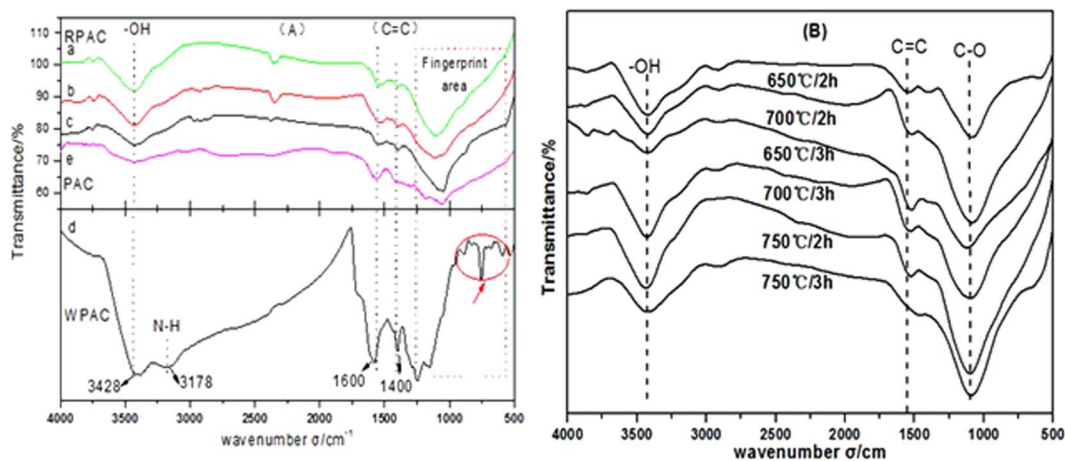


Figure 2. Characteristic of WPAC (A) FTIR of WPAC before and after regeneration; (B) FTIR of WPAC under different regeneration conditions. a: 650 °C, 2 h; b: 650 °C, 3 h; c: 700 °C, 2 h, d: WPAC; e: PAC.

Peak position/cm ⁻¹	Functional group	Before regeneration	After regeneration
3428 cm ⁻¹	-OH	Strong	Weaken
3178 cm ⁻¹	-NH-/-NH ₂ -	Strong	Disappear
1600–1400 cm ⁻¹	C=C	Strong	Weaken
1000–1300 cm ⁻¹	C-O	Strong	Weaken
500–1000 cm ⁻¹ (fingerprint)	—	Complicated	Disappear

Table 1. Analysis of the peaks of FTIR spectra.

Characteristic of WPAC under different regeneration conditions. Changes in surface functional groups are also reflected by the FTIR spectra. The FTIR spectra of WPAC before and after regeneration are presented in Fig. 2. The relevant peaks attributed to special functional groups and compounds are summarized in Table 1. The peaks at wave numbers of 3428, 3178, 1400–1600, 500–1000 cm⁻¹ showed the surface carbon structure of the WPAC. This structure consists of chain hydrocarbons and functional groups such as anthranilic acid, methyl anthranilate and methyl ortho-chlorobenzoate. Peaks at 3178 cm⁻¹ and 500–1000 cm⁻¹ were disappeared. Peaks at 3428 cm⁻¹, 1600–1400 cm⁻¹ and 1000–1300 cm⁻¹ were weakened. It indicated that the anthranilic acid and anthranilic acid methyl ester adsorbed on the WPAC had been effectively decomposed after pyrolysis regeneration. Meanwhile, the spectra were very sensitive to the changes of molecular structure in the fingerprint area. The peaks disappeared in the fingerprint area indicated that the organic matters adsorbed by the PAC had been decomposed. It also could be seen that the organic matters adsorbed on the WPAC had been effectively decomposed at 650 °C after 2 h regeneration.

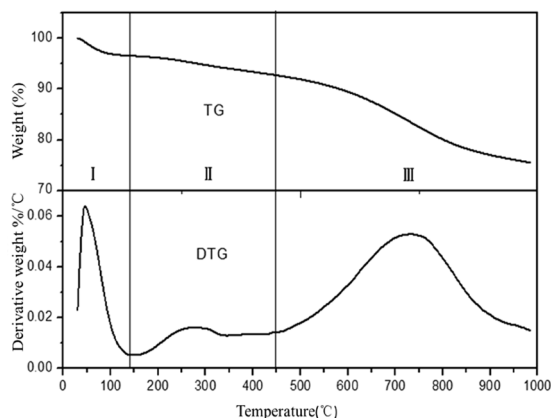


Figure 3. TG/DTG curve of RWPAC.

sample	PAC	WPAC	RWPAC
BET surface area ($\text{m}^2\text{-g}^{-1}$)	1228.6	593.2	1161.4
total pore volume (m^3/g)	1.2380	0.4932	1.2176
t-Plot micropore volume (m^3/g)	0.2545	0.0991	0.2232
Mesoporous volumes (m^3/g)	0.8737	0.3015	0.8026

Table 2. BET surface and pore volume of PAC, WPAC and RWPAC.

Figure 3 showed the TG and DTG pyrolysis profiles of WPAC. The TG-DTG curves showed that mass of the sample was lost gradually and the decomposition process could be divided into three phases: moisture desorption, thermal desorption of organic and inorganic matters adsorbed by activated carbon, and finally carbonization of solid pyrolysis residue.

- (1) The first weight loss step is from 50~110 °C which was due to the water emission. It is well known that some of the water in the sample and the boiling point of the water is relatively low which could be easily stripped under low temperature.
- (2) The second weight loss step is from 200 °C to 350 °C, this step was considered as the dehydration of oxygen containing functional groups.
- (3) The third weight loss step is from 600~800 °C which was the main pyrolysis stage for the pyrolysis of organic compounds adsorbed on the WPAC.

Table 2 showed the BET surface and pore volume of PAC, WPAC and RWPAC. It could be seen that there were obvious differences between WPAC and RWPAC. PAC had a large BET surface which could be reached to 1228.6 m^2/g . While WPAC only had 593.2 m^2/g which was 48.3% of PAC. After 2 h regeneration at 650 °C, BET surface of RWPAC had been recovered to 1161.4 m^2/g which was 94.5% of PAC. Compared with the total pore volume of PAC (1.2380 m^3/g), the total pore volume of WPAC was 0.4932 m^3/g while RWPAC had a total pore volume of 1.2176 m^3/g . RWPAC can keep its porous structure and has a relative high specific surface area after regenerated by pyrolysis method. These results indicated pyrolysis was an effective way to recover the WPAC and the characteristic of WPAC could be recovered which was benefit for re-utilization of WPAC.

Phosphorus adsorption. For evaluation of regenerated WPAC, the adsorption performance of $\text{PO}_4^{3-}\text{-P}$ was investigated. In this study, the adsorption capacity of PAC, WPAC and RWPAC was tested by varying the initial concentration of phosphorus (P) (20 °C). Figure 4 show the general trend is such that the adsorption capacity increases with the increase in the initial P concentration until reaching the saturated state. The maximum adsorption capacity of PAC, WPAC and RWPAC were 16.86 $\text{mgPO}_4^{3-}\text{-P}/\text{g}$, 8.70 $\text{mgPO}_4^{3-}\text{-P}/\text{g}$, and 13.27 $\text{mgPO}_4^{3-}\text{-P}/\text{g}$ respectively.

Adsorption isotherms and kinetic modeling. *Adsorption isotherms.* In order to evaluate the difference in regeneration on enhancing the adsorption performance of WPAC, it was necessary to develop a similar equilibrium to provide a better comparison and understanding of the adsorption process. For this study, the isotherm parameters of two models calculated from the slope and the intercept of the plots were given in Table 3. The results indicated that the adsorption of PAC, WPAC and RWPAC on P could be well described by Langmuir model ($R^2 > 0.943$) compared with the Freundlich model ($R^2 > 0.83$). The Langmuir isotherm model is based on the assumption that all adsorption sites are alike and equally energetic, making the surface homogeneous¹⁶. The $\text{PO}_4^{3-}\text{-P}$ adsorption mechanism by PAC was single-layer adsorption. From the fitting of experimental data using the Langmuir isotherm, it was found that there were consistent between the model-fitted and

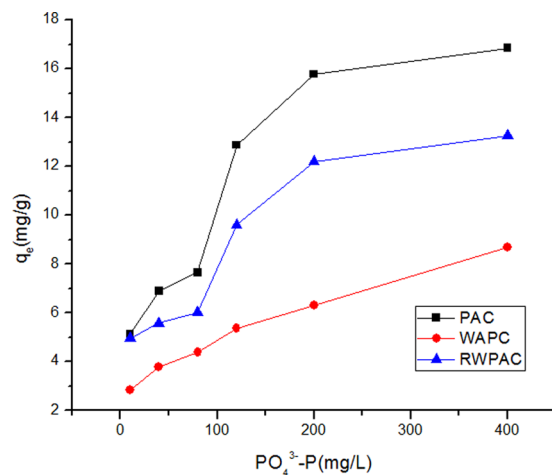


Figure 4. Adsorption performance of PAC, WPAC and RWPAC on phosphorus (P).

Object	Langmuir parameter			Freundlich parameter		
	q_{max} (mg/g)	k_l (L/mg)	R^2	k_f (mg/g)	$1/n$	R^2
PAC	19.72	0.014	0.9504	2.03	0.1188	0.8993
WPAC	9.65	0.014	0.9496	1.99	0.3586	0.8609
RWPAC	15.31	0.015	0.9479	2.13	0.2998	0.8337

Table 3. Isotherms parameters of Langmuir and Freundlich models for PAC, WPAC and RWPAC.

experimentally measured adsorption capacities. According to the calculation results of Langmuir model, PAC used in this study had a maximum P adsorption capacity of 19.72 mg/g. It is higher than the results of Li who used the powder activated carbon(PAC) prepared from rice husks as the adsorbent of phosphorus(P) which had a saturated adsorption capacity of 6.93 mg/g¹⁷. The lower specific surface area(BET) of powder activated carbon (886.3 m²/g) resulted in a lower adsorption capacity compared with RWPAC (1161.4 m²/g) in this paper. WPAC had a maximum PO₄³⁻-P adsorption capacity of 9.65 mg/g which was 48.93% of fresh PAC. While RWPAC had a maximum PO₄³⁻-P adsorption capacity of 15.31 mg/g which was 77.64% of PAC. It indicated that the adsorption capacity had been greatly recovered after regeneration.

Adsorption kinetics. To investigate the mechanism involved in the P adsorption onto the PAC, WPAC and RWPAC, the pseudo-second-order kinetic model and the intraparticle model were used for the analysis of P adsorption.

The pseudo-second-order equation is expressed as¹⁸:

$$\frac{t}{q_t} = \frac{1}{k_1 q_e^2} + \frac{1}{q_e} t \quad (5)$$

The intraparticle diffusion equation is expressed as¹⁹:

$$q_t = k_2 t^{1/2} + d \quad (6)$$

where, k_1 and k_2 represented the rate constant of the pseudo-second-order model (g/min mg) and the intraparticle diffusion rate constant (mg/min^{1/2} g), respectively. The q_e and q_t (mg/g) are the quantity of PO₄³⁻-P adsorbed at equilibrium and at time t, respectively, with d as the intercept.

Based on Eqs (5) and (6), the values of k_1 and q_e could be obtained from the straight-line plot for t/q_t against t (Table 4). The kinetics of PAC, WPAC and RWPAC on phosphorus (P) were very fast which could be reached to pseudo-equilibrium in the 3 h. These results confirmed that PAC was an attractive adsorbent which was widely used in wastewater treatments because of its large surface area and well developed pore.

The plots for the pseudo-second-order kinetic and the intraparticle diffusion model fitted with the experimental data for PAC, WPAC and RWPAC were shown in Fig. 5(a) and (b). Comparing the correlation coefficients listed in Table 3, it was found that the adsorption of PO₄³⁻-P by PAC, WPAC and RWPAC could be well described by the pseudo-second-order kinetic model, which has a higher correlation coefficient value ($R^2 > 0.94$). The P adsorbed on the PAC, WPAC and RWPAC involves two stages (surface sorption and intraparticle diffusion). The intraparticle diffusion model can only be applied to describe the first linear stage of PO₄³⁻-P, which is probably due to the boundary-layer diffusion effect, whereas the final linear portion may be due to the intraparticle effect²⁰.

	pseudo-second-order kinetic model			intra-particle model	
	k_1 (g/min mg)	q_e (mg/g)	R^2	k_2 (mg/min ^{1/2} g)	R^2
PAC	0.48	19.05	0.9484	1.0731	0.8934
WPAC	1.6	7.10	0.9870	0.4416	0.9425
RWPAC	0.78	13.46	0.9618	0.7981	0.8826

Table 4. Kinetic matters for P adsorption using pseudo-second-order kinetic model and the intra-particle model.

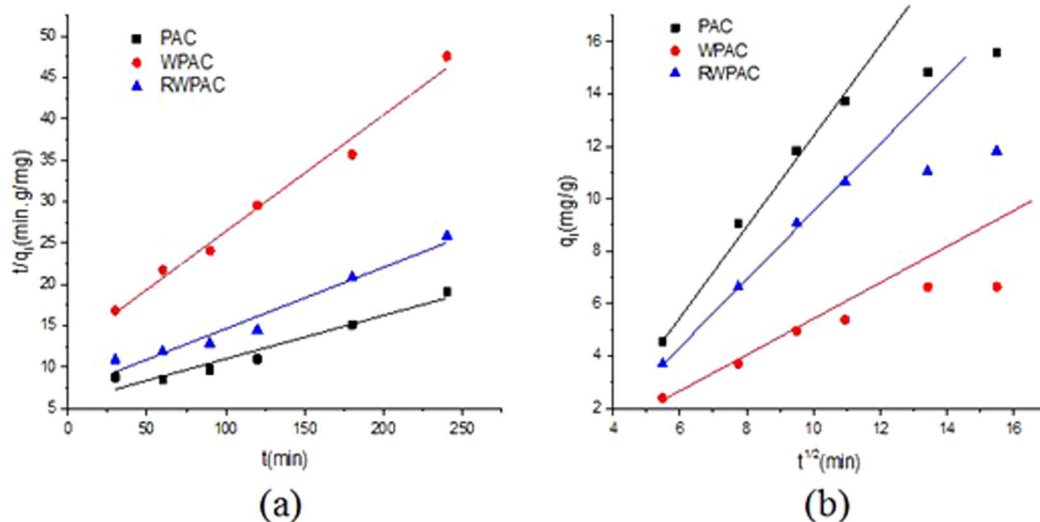


Figure 5. (a) Pseudo-second-order kinetic models for P adsorption by PAC, WPAC and RWPAC. (b) Intraparticle diffusion models for P adsorption by PAC, WPAC and RWPAC.

Benefit of the regeneration by pyrolysis. The WPAC could be regenerated through pyrolysis which had several advantages: first, it cut down the consumption of the coal and the natural resources; secondly, it reduced the secondary pollution by the WPAC; finally, it greatly cut down the cost of wastewater treatment. The energy demands of regeneration was mainly consumed by the pyrolysis furnace. The consumption of electric by pyrolysis furnace was about 40 kwh to regenerate 1 ton WPAC, while the consumption of electric to produce 1 ton PAC was about 160 kwh. It could be seen that the energy demands of regeneration had been greatly decreased which was about 25% of the energy demands required to produce new PAC.

Conclusion

Through this study, it was found that waste power activated carbon could be recovered by pyrolysis regeneration method. The optimum regeneration conditions were 650 °C and 2 h. Under this condition, BET surface of RWPAC had been recovered to 1161.4 m²/g which was 94.5% of PAC. The pyrolysis of WPAC consists three stages: moisture emission, dehydration of oxygen containing functional groups and carbonization. The performance of PO₄³⁻-P adsorption were also studied to evaluate the regeneration process. The PO₄³⁻-P adsorption capacity recovery percentage could increased from 48.93% (WPAC) to 77.64% (RWPAC) of fresh PAC. This regeneration method can recover the characteristic of WPAC to ensure the adsorption capacity and decrease the risk of secondary pollution in the activated carbon regeneration process.

References

- Ma, A. *et al.* Study on regeneration of spent activated carbon by using a clean technology. *Green Processing & Synthesis* **6**(5) (2017).
- Zhan, J. *et al.* Simultaneous regeneration of p -nitrophenol-saturated activated carbon fiber and mineralization of desorbed pollutants by electro-peroxone process. *Carbon* **101**, 399–408 (2016).
- Li, Q., Qi, Y. & Gao, C. Chemical regeneration of spent powdered activated carbon used in decolorization of sodium salicylate for the pharmaceutical industry. *Journal of Cleaner Production* **86**, 424–431 (2015).
- Cabrera-Codony, A., Gonzalez-Olmos, R. & Martin, M. J. Regeneration of siloxane-exhausted activated carbon by advanced oxidation processes. *Journal of Hazardous Materials* **285**, 501–508 (2015).
- Radic, D., Stanojevic, M., Obradovic, M. & Jovovic, A. Thermal analysis of physical and chemical changes occurring during regeneration of activated carbon. *Thermal Science* **21**, 1067–1081 (2016).
- Cazetta, A. L. *et al.* Thermal regeneration study of high surface area activated carbon obtained from coconut shell: Characterization and application of response surface methodology. *Journal of Analytical & Applied Pyrolysis* **101**, 53–60 (2013).
- Meng, J. *et al.* Effect of seed sludge on nitrogen removal in a novel upflow microaerobic sludge reactor for treating piggery wastewater. *Bioresour Technol* **216**, 19–27, <https://doi.org/10.1016/j.biortech.2016.05.034> (2016).
- Wu, D., Li, S. & Wang, N. Microwave regeneration of biological activated carbon. *Journal of Advanced Oxidation Technologies* **20**, 1–10 (2017).

9. Lee, K. M. & Lim, P. E. Bioregeneration of powdered activated carbon in the treatment of alkyl-substituted phenolic compounds in simultaneous adsorption and biodegradation processes. *Chemosphere* **58**, 407 (2005).
10. Jonge, R. J. D., Breure, A. M. & Andel, J. G. V. Bioregeneration of powdered activated carbon (PAC) loaded with aromatic compounds. *Water Research* **30**, 875–882 (1996).
11. Clifford, D., Chu, P. & Lau, A. Thermal regeneration of powdered activated carbon (pac) and pac-biological sludge mixtures. *Water Research* **17**, 1125–1138 (1983).
12. Mao, Q., Zhang, S. & Zhao, M. *et al.* Study on Thermal Conversion of the Waste Oil Absorbin Activated Carbon. *MATEC Web of Conferences* **100**, 04003 (2017).
13. Danon, B., van der Gryp, P., Schwarz, C. E. & Görgens, J. F. A review of dipentene (dl-limonene) production from waste tire pyrolysis. *Journal of Analytical and Applied Pyrolysis* **112**, 1–13, <https://doi.org/10.1016/j.jaap.2014.12.025> (2015).
14. Lu, S. G., Bai, S. Q., Zhu, L. & Shan, H. D. Removal mechanism of phosphate from aqueous solution by fly ash. *Journal of Hazardous Materials* **161**, 95 (2009).
15. Gong, G. *et al.* Preparation of a new sorbent with hydrated lime and blast furnace slag for phosphorus removal from aqueous solution. *Journal of Hazardous Materials* **166**, 714 (2009).
16. Vimonses, V., Lei, S. M., Jin, B., Chow, C. W. K. & Saint, C. Kinetic study and equilibrium isotherm analysis of Congo Red adsorption by clay materials. *Chem. Eng. J.* **148**, 354–364 (2009).
17. Nan, L. & Shan. Preparation of powder activated carbon by rice husks and its adsorption capacity to phosphorus. *Chinese Journal of Environmental Engineering* **7**, 1024–1028 (2013).
18. Qiu, H. *et al.* Critical review in adsorption kinetic models. *Journal of Zhejiang University* **10**, 716–724 (2009).
19. Huang, H. *et al.* Removal of ammonium from swine wastewater by zeolite combined with chlorination for regeneration. *Journal of Environmental Management* **160**, 333–341 (2015).
20. Alshameri, A. *et al.* An investigation into the adsorption removal of ammonium by salt activated Chinese (Hulaodu) natural zeolite: Kinetics, isotherms, and thermodynamics. *Journal of the Taiwan Institute of Chemical Engineers* **45**, 554–564 (2014).

Acknowledgements

This research was supported by Hubei Province excellent Science and Technology Innovation Team Project (NO. T201407).

Author Contributions

Data curation: Hailan Jin. Formal analysis: Wenbo Liu. Investigation: Hang Su. Software: Yao Lu. Writing – original draft: Yi Li. Writing – review & editing: Jianfen Li.

Additional Information

Competing Interests: The authors declare that they have no competing interests.

Publisher's note: Springer Nature remains neutral with regard to jurisdictional claims in published maps and institutional affiliations.



Open Access This article is licensed under a Creative Commons Attribution 4.0 International License, which permits use, sharing, adaptation, distribution and reproduction in any medium or format, as long as you give appropriate credit to the original author(s) and the source, provide a link to the Creative Commons license, and indicate if changes were made. The images or other third party material in this article are included in the article's Creative Commons license, unless indicated otherwise in a credit line to the material. If material is not included in the article's Creative Commons license and your intended use is not permitted by statutory regulation or exceeds the permitted use, you will need to obtain permission directly from the copyright holder. To view a copy of this license, visit <http://creativecommons.org/licenses/by/4.0/>.

© The Author(s) 2018